

1 **PD-L1 expression in equine malignant melanoma and functional effects of PD-L1 blockade**

2

3 Otgontuya Ganbaatar¹, Satoru Konnai^{1,2,*}, Tomohiro Okagawa², Yutaro Nojima¹, Naoya
4 Maekawa², Erina Minato³, Atsushi Kobayashi³, Ryo Ando⁴, Nobuya Sasaki⁵, Daisuke Miyakosi⁶,
5 Osamu Ichi⁷, Yukinari Kato^{8,9}, Yasuhiko Suzuki^{2,10}, Shiro Murata^{1,2}, Kazuhiko Ohashi^{1,2}

6

7 ¹Department of Disease Control, Faculty of Veterinary Medicine, Hokkaido University, Sapporo,
8 Japan; ²Department of Advanced Pharmaceutics, Faculty of Veterinary Medicine, Hokkaido
9 University, Sapporo, Japan; ³Department of Veterinary Clinical Medicine, Faculty of Veterinary
10 Medicine, Hokkaido University, Sapporo, Japan; ⁴Laboratory of Veterinary Pathology, School of
11 Veterinary Medicine, Kitasato University, Towada, Japan; ⁵Laboratory of Laboratory Animal
12 Science and Medicine, School of Veterinary Medicine, Kitasato University, Towada, Japan;
13 ⁶Mitsubishi Animal Medical Center, NOSAI minami, Shinihidaka, Japan; ⁷Department of Basic
14 Veterinary Sciences, Faculty of Veterinary Medicine, Hokkaido University, Sapporo, Japan;
15 ⁸Department of Antibody Drug Development, Tohoku University Graduate School of Medicine,
16 Sendai, Japan; ⁹New Industry Creation Hatchery Center, Tohoku University, Sendai, Japan;
17 ¹⁰Division of Bioresources, Research Center for Zoonosis Control, Hokkaido University, Sapporo,
18 Japan.

19

20 Running title: Identification and function of equine PD-1 and PD-L1

21

22 *Correspondence: Satoru Konnai, konnai@vetmed.hokudai.ac.jp

23 **Abstract**

24 Programmed death-1 (PD-1) is an immunoinhibitory receptor expressed on exhausted T cells
25 during chronic illness. Interaction of PD-1 with its ligand PD-ligand 1 (PD-L1) delivers inhibitory
26 signals and impairs proliferation, cytokine production, and cytotoxicity of T cells. We reported
27 that the PD-1/PD-L1 pathway is closely associated with T-cell exhaustion and disease progression
28 in bovine chronic infections and canine tumors. Moreover, we found that blocking antibodies
29 targeting PD-1 and PD-L1 restore T-cell functions and may be used in immunotherapy in cattle
30 and dogs. However, the immunological role of the PD-1/PD-L1 pathway remains unclear for
31 chronic equine diseases, including tumors. In this study, we identified nucleotide sequences of
32 equine PD-1 (EqPD-1) and PD-L1 (EqPD-L1) and investigated the role of anti-bovine PD-L1
33 monoclonal antibodies (mAbs) against EqPD-L1 using *in vitro* assays. We also evaluated the
34 expression of PD-L1 in tumor tissues of equine malignant melanoma (EMM).

35 The amino acid sequences of EqPD-1 and EqPD-L1 share a high identity and similarity with
36 homologs from other mammalian species. Two clones of the anti-bovine PD-L1 mAbs recognized
37 EqPD-L1 in flow cytometry, and one of these cross-reactive mAbs blocked the binding of equine
38 PD-1/PD-L1. Importantly, PD-L1 expression was confirmed in EMM tumor tissues by
39 immunohistochemistry. A cultivation assay revealed that PD-L1 blockade enhanced the
40 production of Th1 cytokines in equine immune cells.

41 These results suggest that our anti-PD-L1 mAbs may be useful for investigating the expression
42 and role of the equine PD-1/PD-L1 pathway. Further research is required to discover the
43 immunological role of PD-1/PD-L1 in chronic equine diseases and elucidate a future application
44 in immunotherapy for horse.

45 **Keywords:** horse, PD-1, PD-L1, IFN- γ , T cells, chronic diseases, melanoma

46 **Introduction**

47 Programmed cell death-1 (PD-1) is an immunoinhibitory receptor, which is expressed on activated
48 and exhausted T cells [1]. Its ligand programmed death ligand 1 (PD-L1) is expressed on immune
49 cells, including antigen-presenting cells, and tumor cells [1]. The interaction of PD-1 and PD-L1
50 suppresses the activation signal mediated by T-cell receptors and inhibits effector functions of T
51 cells, such as cytokine production and cell proliferation [1]. This pathway is invaluable for
52 regulating excessive immune responses. In cancers, however, tumor cells utilize the suppression
53 of T cells mediated by PD-1/PD-L1 to avoid anti-tumor immune responses [1]. In human medicine,
54 the blocking antibodies targeting PD-1 or PD-L1 have been leveraged for treatment of various
55 types of cancers and resulted in remarkable outcomes with 20%–90% response rates in multiple
56 clinical trials [1].

57 Equine malignant melanoma (EMM) is a common neoplasm among aged gray horses, which
58 results in dermal tumors at multiple sites [2]. A previous study reported that around 80% of aged
59 gray horses developed dermal melanoma and predicted that all gray horses would develop this
60 tumor as they reach old age [3]. Cellular immune response is critical for the eradication of
61 melanoma, but several mechanisms have been propounded to limit anti-tumor immunity in EMM
62 based on the findings for human malignant melanoma [4]. However, no studies on immune evasion
63 mechanisms in EMM have yet been done, and immune exhaustion mediated by PD-1 and PD-L1
64 has not been investigated in horses.

65 In our previous research, we established anti-bovine PD-L1 monoclonal antibodies (mAbs) [5].
66 We found that PD-1 and PD-L1 play critical roles in immune exhaustion and disease progression
67 in bovine chronic infections [6–10] and in canine cancers including malignant melanoma [11, 12].
68 Importantly, we noted that the PD-1/PD-L1 blockade enhances T-cell responses in cattle and dogs

69 and exhibits therapeutic effects in bovine chronic infections and canine malignant melanoma [6–
70 10, 13–17].

71 So far, there are no reports on genetic information, expression, and function of PD-1/PD-L1 in
72 horses. Furthermore, the role of the PD-1/PD-L1 pathway in EMM remains unclear. Based on the
73 findings of our previous studies, we hypothesized that PD-1 and PD-L1 may provide potential
74 targets for immunotherapy against EMM. Hence, in this study, we identified nucleotide sequences
75 of equine PD-1 (EqPD-1) and PD-L1 (EqPD-L1), evaluated the blocking effects of our anti-bovine
76 PD-L1 mAbs against EqPD-L1, and confirmed the expression of PD-L1 on EMM.

77

78 **Materials and Methods**

79 **Horse blood samples and cell preparation**

80 Heparinized blood samples were collected from Thoroughbred horses in farms and veterinary
81 hospitals in Hokkaido, Japan. Peripheral blood mononuclear cells (PBMCs) were purified using
82 density gradient centrifugation on Percoll (GE Healthcare, Little Chalfont, UK), washed three
83 times with phosphate-buffered saline (PBS), and suspended in PBS. All experimental procedures
84 were conducted following approval from the local committee for animal studies according to the
85 Hokkaido University (17-0024). Informed consent was obtained from all owners.

86 **Cloning of cDNA encoding of equine PD-1 and PD-L1**

87 Equine PBMCs (4×10^6 cells) were cultivated with 20 ng/mL of phorbol 12-myristate acetate
88 (PMA; Sigma–Aldrich, St. Louis, MO, USA) and 1 $\mu\text{g}/\text{mL}$ of ionomycin (Sigma–Aldrich) in
89 RPMI 1640 medium (Sigma–Aldrich) supplemented with 10% heat-inactivated fetal bovine serum
90 (FBS) (Thermo Fisher Scientific, Waltham, MA, USA), 2 mM of L-glutamine, 100 U/mL of
91 penicillin, and 100 $\mu\text{g}/\text{mL}$ of streptomycin (Thermo Fisher Scientific) at 37°C with 5% CO₂ for 24
92 h.

93 Total RNA was isolated from cultivated PBMCs using of TRI Reagent (Molecular Research
94 Center, Cincinnati, OH, USA) according to the manufacturer's instructions. Residual DNA was
95 removed from RNA samples by treatment with Deoxyribonuclease I (Thermo Fisher Scientific).
96 cDNA was synthesized from 1 μg of total RNA with PrimeScript Reverse Transcriptase (Takara
97 Bio, Otsu, Japan) and oligo(dT) primer according to the manufacturer's instructions.

98 Gene-specific primers were designed to amplify EqPD-1 and EqPD-L1 genes, based on the
99 sequences from horses available on GenBank (XM_005610777 and XM_001492842). EqPD-1
100 and EqPD-L1 cDNAs were amplified by PCR using TaKaRa Ex Taq (Takara Bio) and specific

101 primers (Supplementary Table 1). The PCR products were purified using a FastGene Gel/PCR
102 Extraction Kit (Nippon Genetics, Tokyo, Japan), and cloned into the pGEM-T Easy Vector
103 (Promega, Madison, WI, USA). They were transferred into *E. coli* HST08 Premium Competent
104 Cells (Takara Bio) and plated onto LB agar plates (Sigma–Aldrich) containing X-gal (Takara Bio)
105 and ampicillin (Sigma–Aldrich). The purified plasmid clones were sequenced using a GenomeLab
106 GeXP Genetic Analysis System (SCIEX, Framingham, MA, USA). The established sequences
107 were aligned, and an unrooted neighbor-joining tree was constructed using MEGA software
108 program version 7.0 [17].

109 **Preparation of EqPD-1- and EqPD-L1-expressing cells**

110 cDNAs encoding EqPD-1 and EqPD-L1 were amplified by PCR using gene-specific primers with
111 restriction enzyme cleavage sites (Supplementary Table 1) and subcloned into the multicloning
112 site of pEGFP-N2 (Clontech, Palo Alto, CA, USA).

113 COS-7 cells were cultured in RPMI 1640 medium (Sigma–Aldrich) supplemented with 10% heat-
114 inactivated FBS (Thermo Fisher Scientific), 2 mM of L-glutamine, 100 U/mL of penicillin, and
115 100 µg/mL of streptomycin (Thermo Fisher Scientific) at 37°C and 5% CO₂. The cells were
116 transfected with purified plasmids using Lipofectamine 3000 Reagent (Thermo Fisher Scientific)
117 and cultivated for 48 h after transfection. The cellular localization of EqPD-1-EGFP and EqPD-
118 L1-EGFP was then confirmed using the ZOE Fluorescent Cell Imager (Bio-Rad, Hercules, CA,
119 USA).

120 **Expression and purification of soluble equine PD-1 and PD-L1 proteins**

121 Soluble forms of EqPD-1 and EqPD-L1 proteins fused with rabbit IgG Fc region (EqPD-1-Ig and
122 EqPD-L1-Ig) were obtained by amplifying cDNAs encoding the extracellular domain fragments
123 of EqPD-1 and EqPD-L1 with signal sequences by PCR with gene-specific primers with restriction

124 enzyme cleavage sites (Supplementary Table 1). The amplicons were subcloned into the
125 multicloning site of pCXN2.1(+) (kindly provided by Dr. T. Yokomizo, Juntendo University,
126 Japan) [19] with the gene cassette encoding the Fc region of rabbit IgG. Transient cell lines
127 expressing EqPD-1-Ig and EqPD-L1-Ig were established with the use of an Expi293 Expression
128 System (Thermo Fisher Scientific). Expi293F cells were transfected with pCXN2.1(+)-EqPD-1-
129 Ig and pCXN2.1(+)-EqPD-L1-Ig using Expifectamine (Thermo Fisher Scientific) and cultivated
130 with shaking in Expi293 medium (Thermo Fisher Scientific) at 37°C and 125 rpm with 8% CO₂
131 for 7 days.

132 Purification of EqPD-1-Ig and EqPD-L1-Ig from the culture supernatants was achieved by affinity
133 chromatography with an Ab-Capcher ExTra (ProteNova, Kagawa, Japan). The buffer was
134 exchanged with PBS by size exclusion chromatography using a PD-10 Desalting Column (GE
135 Healthcare). The purity of EqPD-1-Ig and EqPD-L1-Ig was confirmed by sodium dodecyl sulfate-
136 polyacrylamide gel electrophoresis (SDS-PAGE) in reducing or nonreducing conditions using
137 SuperSep Ace 5%–20% gradient polyacrylamide gel (FUJIFILM Wako Pure Chemical, Osaka,
138 Japan) and 2 × Laemmli Sample Buffer (Bio-Rad).

139 Precision Plus Protein All Blue Standard (Bio-Rad) was used as a molecular-weight size marker.
140 The proteins were visualized with Quick-CBB (FUJIFILM Wako Pure Chemical), and protein
141 concentrations were measured by ultraviolet absorbance at 280 nm with a NanoDrop 8000
142 Spectrophotometer (Thermo Fisher Scientific).

143 **Binding assay of EqPD-1 and EqPD-L1**

144 Binding of EqPD-1-Ig and EqPD-L1-Ig to COS-7 cells expressing EqPD-L1-EGFP and EqPD-1-
145 EGFP were investigated using flow cytometry. EqPD-L1-EGFP cells or EqPD-1-EGFP cells were
146 incubated with 10 µg/mL of biotinylated EqPD-1-Ig or EqPD-L1-Ig, respectively, at 37°C for 30

147 min. Biotinylated rabbit control IgG (Southern Biotech, Birmingham, AL, USA) was used as a
148 negative control. EqPD-1-Ig, EqPD-L1-Ig, and rabbit control IgG were biotinylated using a
149 Lightning-Link Rapid Type A Biotin Conjugation Kit (Innova Biosciences, Cambridge, UK).
150 Cells were washed with PBS containing 1% bovine serum albumin (BSA; Sigma–Aldrich) and
151 labeled using APC-conjugated streptavidin (BioLegend, San Diego, CA, USA) at 25°C for 30 min.
152 After rewashing, cells were immediately analyzed by FACS Verse (BD Biosciences, San Jose,
153 CA, USA).

154 **Cross-reactivity assay of anti-bovine PD-L1 mAbs against EqPD-L1**

155 EqPD-L1-EGFP cells were incubated with four clones of anti-bovine PD-L1 mAbs (4G12-C1, rat
156 IgG_{2a}; 5A2-A1, rat IgG₁; 6C11-3A11, rat IgG_{2a}; 6G7-E1, rat IgM) [5, 20] at 25°C for 20 min to
157 analyze the binding ability of anti-bovine PD-L1 mAbs to EqPD-L1. Rat IgG₁ (R3-34, BD
158 Biosciences, San Jose, CA, USA), rat IgG_{2a} (R35-95, BD Biosciences), and rat IgM isotype
159 controls (R4-22, BD Biosciences) were used for negative control staining. Cells were washed with
160 1% BSA-PBS and labeled with APC-conjugated goat anti-rat immunoglobulin antibody (Southern
161 Biotech) at 25°C for 20 min. After rewashing, cells were immediately analyzed by FACS Verse
162 (BD Biosciences).

163 Fresh and stimulated equine PBMCs were analyzed by flow cytometry to analyze the
164 binding ability of anti-bovine PD-L1 mAbs to equine immune cells. Equine PBMCs (4×10^6 cells)
165 were stimulated in cultivation with 20 ng/mL of PMA (Sigma–Aldrich) and 1 µg/mL of ionomycin
166 (Sigma–Aldrich) for 24 h, as described above. Fresh and stimulated PBMCs were incubated with
167 PBS supplemented with 10% goat serum (Thermo Fisher Scientific) at room temperature for 15
168 min to prevent nonspecific reactions. Cells were washed and stained with anti-PD-L1 mAbs (5A2-
169 A1, rat IgG₁; 6C11-3A11; rat IgG_{2a}) [5, 20] at room temperature for 30 min. Rat IgG₁ (R3-34, BD

170 Biosciences) and rat IgG_{2a} isotype controls (R35-95, BD Biosciences) were used for negative
171 control staining. Cells were washed with PBS containing 1% BSA (Sigma–Aldrich) and labeled
172 with APC-conjugated anti-rat Ig antibody (Southern Biotech) at room temperature for 30 min.
173 After rewashing, cells were immediately analyzed by FACS Verse (BD Biosciences).

174 **Blockade assay of EqPD-1/EqPD-L1 interaction**

175 Blocking assays were conducted on microplates using EqPD-1-Ig and EqPD-L1-Ig to analyze the
176 ability of the anti-PD-L1 mAbs to block PD-1/PD-L1 binding. MaxiSorp Immuno Plates (Thermo
177 Fisher Scientific) were coated with EqPD-1-Ig (1 µg/mL) in carbonate-bicarbonate buffer (Sigma–
178 Aldrich) and blocked with SuperBlock T20 (PBS) Blocking Buffer (Thermo Fisher Scientific).
179 Biotinylated EqPD-L1-Ig was preincubated with anti-PD-L1 mAb 5A2-A1 (rat IgG₁) [5], 6C11-
180 3A11 (rat IgG_{2a}) [20], rat IgG₁ isotype control (R3-34, BD Biosciences), or rat IgG_{2a} isotype
181 control (R35-95, BD Biosciences) at various concentrations (0, 1.25, 2.5, 5.0, 7.5, 10 µg/mL) at
182 37°C for 30 min. The preincubated reagents were added to the microplates and incubated at 37°C
183 for a further 30 min. EqPD-L1-Ig binding was detected using horseradish peroxidase-conjugated
184 Neutravidin (Thermo Fisher Scientific) and TMB One Component Substrate (Bethyl Laboratories,
185 Montgomery, TX, USA). Optical density at 450 nm was measured by a microplate reader MTP-
186 900 (Corona Electric, Hitachinaka, Japan). Three independent experiments were each performed
187 in duplicate.

188 **Immunohistochemical assay of PD-L1**

189 Tumor tissues from four horses bearing EMM were immunohistochemically stained
190 (Supplementary Table 2). The tissues were fixed in formalin, embedded into paraffin wax and cut
191 into 4-µm-thick sections. The dried sections were deparaffinized in xylene and hydrated through
192 graded alcohols. Melanin was bleached from the sections with using 0.25% potassium

193 permanganate and 2% oxalic acid. Antigen retrieval was achieved using 0.01 M citrate buffer (pH
194 6.0) by microwave heating. Endogenous peroxidase activity was blocked by incubating the
195 sections in methanol containing 0.3% hydrogen peroxide. The sections were incubated with or
196 without anti-PD-L1 mAb (6C11-3A11, rat IgG_{2a}) [20] at 4°C overnight, followed by detection
197 using Vectastain Elite ABC Rat IgG kit (Vector Laboratories, Burlingame, CA, USA). The
198 immunoreaction was visualized using 3,3'-diaminobenzidine tetrahydrochloride. All
199 immunostained sections were examined under an optical microscope.

200 **Immunoactivation assay using equine PBMCs**

201 To determine the effects of inhibiting the PD-1/PD-L1 interaction on equine immune cells, equine
202 PBMCs were cultured with 10 µg/mL of anti-PD-L1 mAb (6C11-3A11, rat IgG_{2a}) [20] or rat IgG_{2a}
203 control (Bio X Cell, West Lebanon, NH, USA) in the presence of 0.1 µg/mL of Staphylococcal
204 enterotoxin B (Sigma–Aldrich) at 37°C with 5% CO₂ for three days. All cell cultures were grown
205 in 96-well round-bottomed plates (Corning Inc., Corning, NY, USA) containing 4×10^5 PBMCs
206 in 200 µl of RPMI 1640 medium (Sigma–Aldrich) supplemented with 10% heat-inactivated FBS,
207 2 mM of L-glutamine, 100 U/mL of penicillin, and 100 µg/mL of streptomycin (Thermo Fisher
208 Scientific). Cytokine concentrations in the culture supernatants were determined using an Equine
209 IFN-γ ELISA Development Kit (Mabtech, Nacka Strand, Sweden) and an Equine IL-2 DuoSet
210 ELISA (R&D Systems, Minneapolis, MN, USA). Measurements were performed in duplicate
211 according to the manufacturer's protocol.

212 **Statistical analysis**

213 Significant differences were identified using Wilcoxon signed-rank test or Tukey's test. All
214 statistical tests were performed using the MEPHAS ([http://www.gen-info.osaka-](http://www.gen-info.osaka-u.ac.jp/MEPHAS/)
215 [u.ac.jp/MEPHAS/](http://www.gen-info.osaka-u.ac.jp/MEPHAS/)) statistical analysis program. Statistical significance was set as $p < 0.05$.

216 **Results**

217 **Molecular cloning and sequence analysis of equine PD-1/PD-L1**

218 Figs 1A and 2A show the putative amino acid sequences of EqPD-1 and EqPD-L1, respectively.
219 EqPD-1 and EqPD-L1 consist of a putative signal peptide, an extracellular region, a
220 transmembrane region, and an intracellular region. These were expected to be type I
221 transmembrane proteins as orthologues in other species. A conserved domain search identified an
222 immunoglobulin variable (IgV)-like domain in the extracellular regions of EqPD-1. IgV-like and
223 immunoglobulin constant (IgC)-like domains were observed in the extracellular regions of EqPD-
224 L1. The intracellular region of EqPD-1 contained two structural motifs, an immunoreceptor
225 tyrosine-based inhibitory motif (ITIM) and an immunoreceptor tyrosine-based switch motif
226 (ITSM). Phylogenetic analyses revealed that EqPD-1 and EqPD-L1 were clustered in a group
227 comprising Artiodactyla and Carnivora (Figs 1B and 2B). EqPD-1 had 70.4%, 69.0%, 75.6%,
228 69.2%, and 58.7% amino acid similarities to pig, cattle, dog, human, and mouse respectively
229 (Table 1). EqPD-L1 amino acid similarities to pig, cattle, dog, human, and mouse were 81.5%,
230 80.9%, 83.7%, 79.0%, and 67.9%, respectively (Table 2).

231 **Interaction of EqPD-1 and EqPD-L1**

232 We evaluated the cellular localization of EqPD-1-EGFP and EqPD-L1-EGFP proteins in the
233 overexpressed COS-7 cell lines and found them to be localized on the cell surface (Fig 3A). We
234 developed soluble recombinant EqPD-1-Ig and EqPD-L1-Ig in the Expi293 Expression System to
235 analyze interactions of EqPD-1 and EqPD-L1 proteins. EqPD-1-Ig and EqPD-L1-Ig were
236 successfully purified from culture supernatants and confirmed to be dimerized by disulfide bonds
237 in the hinge region of rabbit IgG (Fig 3B).

238 We used flow cytometry to analyze the interactions of EqPD-1-Ig or EqPD-L1-Ig with EqPD-L1-
239 EGFP- or EqPD-1-EGFP-expressing cells, respectively. This revealed that EqPD-1-Ig binding to
240 EqPD-L1-EGFP-expressing cells depends on the expression level of EqPD-1-EGFP (Fig 3C).
241 Additionally, we confirmed that EqPD-L1-Ig binds to EqPD-1-EGFP-expressing cells in an
242 expression dependent manner (Fig 3C).

243 **Cross-reactivity of anti-bovine PD-L1 mAbs against EqPD-L1**

244 We evaluated cross reactivity of our previously established anti-bovine PD-L1 mAbs [5, 20]
245 against EqPD-L1 and found that two out of the four tested mAbs (5A2-A1 and 6C11-3A11)
246 detected EqPD-L1-EGFP overexpressed on COS-7 cells (Fig 4A). Of all the tested mAbs, 6C11-
247 3A11 showed the strongest binding to EqPD-L1-EGFP-expressing cells (Fig 4A). We also tested
248 the reactivity of 5A2-A1 and 6C11-3A11 mAbs against fresh and stimulated equine PBMCs and
249 found that 6C11-3A11 mAb binds to both of fresh and stimulated PBMCs (Fig 4B and C). PD-L1
250 expression was upregulated on PBMCs through stimulation with PMA and ionomycin (Fig 4C).

251 **Inhibition of EqPD-1/EqPD-L1 binding by anti-PD-L1 mAbs**

252 We used ELISA to investigate whether the cross-reactive anti-bovine PD-L1 mAbs interfered with
253 the interaction of EqPD-1/EqPD-L1. The 6C11-3A11 mAb, blocked the binding of EqPD-L1-Ig
254 to EqPD-1-Ig in a dose-dependent manner, but the 5A2-A1 did not (Fig 5).

255 **Immunohistochemical analysis of PD-L1 in EMM**

256 PD-L1 has been shown to be upregulated on many types of tumors in dogs and humans [11, 12,
257 21]. Among canine malignant cancers, malignant melanoma has the highest positive rates for PD-
258 L1 expression [11]. Gray horses are susceptible to melanoma and around 80% of them develop
259 EMM in their lifetimes [3]. We hypothesized that PD-L1 plays a role in the development of EMM.

260 Hence, we analyzed the expression of PD-L1 in tumor tissues of EMM by immunohistochemistry.

261 PD-L1 was detected in all EMM samples ($n = 4$, Fig 6B).

262 **Immune activation in equine PBMCs by anti-PD-L1 mAb**

263 We analyzed immune activation effects by PD-1/PD-L1 inhibition in the PBMC culture assays

264 using anti-PD-L1 blocking mAb, 6C11-3A11. We found that PD-L1 blockade by the mAb 6C11-

265 3A11 significantly induced IFN- γ production by equine PBMCs under stimulation with SEB (Fig

266 7A). Additionally, production of IL-2 was increased by PD-L1 inhibition (Fig 7B). These results

267 indicate that PD-1/PD-L1 blockade enhanced Th1 cytokine production in equine PBMCs,

268 suggesting that the anti-PD-L1 blocking antibody may have an application as an

269 immunomodulatory agent for horses.

270

271 **Discussion**

272 The greater longevity of the horse population has increased the risks of chronic diseases, such as
273 laminitis, pituitary pars intermedia dysfunction, recurrent airway obstruction, osteoarthritis, and
274 neoplasia, and increased multimorbidity in horses [22, 23]. However, few treatments are available
275 for chronic diseases in horses, including malignant tumors. Hence, new treatment options are being
276 sought.

277 Malignant melanoma is one of the most common cutaneous neoplasia in horses [24] Surgical
278 treatment is a successful in the early stages of disease, but it is not feasible in cases with multiple
279 tumor burdens and metastases. Although a number of systemic treatments have been tested, no
280 effective systemic therapy is currently available for EMM. To overcome the current situation,
281 novel therapeutic strategies, including immunotherapy, are warranted for EMM.

282 A variety of immunotherapies have been developed and tested in clinical trials to treat tumors in
283 humans, and immune checkpoint inhibitors such as anti-PD-1 and anti-PD-L1 antibodies are
284 currently used with notable success for the treatment of multiple human cancers [25, 26]. Blockade
285 therapy using anti-PD-L1 antibody resulted in long-term tumor regression and prolonged
286 progression free survival in advanced melanoma in humans [26]. Based on these advancements in
287 human medicine, immune checkpoint inhibitors may reasonably be expected to yield equally
288 promising results in the treatment of EMM [4]. However, as yet no studies have been conducted
289 on the PD-1/PD-L1 pathway in horses.

290 Our recent research revealed that the PD-1/PD-L1 pathway plays critical roles in immune
291 exhaustion and disease progression in bovine chronic infections and canine malignant cancers [6–
292 16]. Moreover, we established anti-PD-L1 and anti-PD-1 blocking antibodies for therapeutic
293 application in cattle and dogs [13–15]. Clinical studies have confirmed the antiviral, antibacterial,

294 and antitumoral effects of antibody treatments [13–17]. However, the blockade effect of the PD-
295 1/PD-L1 pathway had not been tested in horses. Hence, we aimed to identify nucleotide sequences
296 of EqPD-1 and EqPD-L1 and evaluate the function of our anti-bovine PD-L1 mAbs using *in vitro*
297 assays.

298 We found that one of the anti-bovine PD-L1 mAbs (6C11-3A11) recognized EqPD-L1 strongly,
299 blocked the interaction of EqPD-1/EqPD-L1 and enhanced the Th1 cytokine response *in vitro*.
300 This anti-PD-L1 mAb may be used to aid investigation into the expression and immunological
301 function of PD-L1 in future horse studies. Additionally, we discovered that PD-L1 is expressed in
302 EMM tumor tissues. Further studies are required to analyze expression of PD-L1 in other horse
303 tumors and chronic diseases.

304 The mechanism of PD-L1 upregulation during EMM progression has yet to be elucidated.
305 Generally, PD-L1 expression is regulated by a substantial number of mediators including
306 inflammatory cytokine signaling, oncogenic signaling, microRNAs, genetic alteration of the PD-
307 L1 locus, and post-translational regulators [27]. In gray horses, a gene duplication in intron 6 of
308 *STX17* (synataxin 17) contributes a *cis*-acting regulatory mutation resulting in a very high
309 incidence of EMM [28]. This gene duplication induces constitutive activation of the extracellular
310 signal-regulated kinase (ERK) pathway and melanomagenesis in EMM [29, 30]. The MEK-ERK
311 signaling pathway regulates PD-L1 gene expression via crosstalk with inflammatory cytokine
312 signaling including the IFN- γ -STAT1 pathway [31–33]. Hence, the regulatory mechanism of PD-
313 L1 expression in gray horses merits investigating as a natural model of tumorigenesis.

314 Our results indicate that the PD-1/PD-L1 pathway offers a potential target for immunotherapy
315 against EMM. In future immunotherapy applications, blocking antibodies should be engineered
316 into suitable forms for administration to horses. Chimeric antibodies, for instance, may facilitate

317 clinical trial research into the clinical efficacy of anti-PD-L1 antibody in the treatment of EMM.

318 Further research is required to develop this novel immunotherapy strategy in horses.

319

320 **Author Contributions**

321 SK, TO, NM, SM, and KO: designed the work; GO, TO, YN, EM, and AK,: performed the
322 experiments; RA, NS, DM, OI, YK, and YS: provided intellectual input, field samples, laboratory
323 materials, reagents, and/or analytic tools; GO, SK, TO, and AK: acquired, analyzed, and
324 interpreted the data; GO and SK: wrote the manuscript; SK, TO, NM, AK, NS, DM, OI, YK, YS,
325 SM, KO: revised the manuscript; all authors: approved the final version of the manuscript.

326

327 **Funding**

328 This work was supported by JSPS KAKENHI grant number 19KK0172 [to S.K.] and 19H03114
329 [to S.K.], grants from the Project of the NARO, Bio-oriented Technology Research Advancement
330 Institution (Research Program on Development of Innovative Technology 26058 BC [to S.K.] and
331 AMED under grant number JP20am0101078 [to Y.K.]. The funders had no role in study design,
332 data collection and analysis, decision to publish, or preparation of the manuscript.

333

334 **Acknowledgments**

335 We are grateful to Dr. Hideyuki Takahashi, Dr. Yasuyuki Mori, and Dr. Tomio Ibayashi for
336 valuable advice and discussions. We would like to thank Enago (www.enago.jp) for the English
337 language review.

338

339 **References**

- 340 1. Bardhan K, Anagnostou T, Boussiotis VA. The PD1: PD-L1/2 pathway from discovery to
341 clinical implementation. *Front Immunol.* 2016;7: 550. doi:10.3389/fimmu.2016.00550
- 342 2. Valentine BA. Equine melanocytic tumors: a retrospective study of 53 horses (1988 to
343 1991). *J Vet Intern Med.* 1995;9: 291–297. doi:10.1111/j.1939-1676.1995.tb01087.x
- 344 3. Mcfadyean J. Equine melanomatosis. *J Comp Pathol Ther.* 1933;46: 186–204.
345 doi:10.1016/s0368-1742(33)80025-7
- 346 4. Cavalleri J-MV, Mählmann K, Schuberth H-J, Feige K. Prospect for immunological
347 therapies of the equine malignant melanoma. *Pferdeheilkunde.* 2015;31: 448–459.
348 doi:10.21836/PEM20150504
- 349 5. Ikebuchi R, Konnai S, Okagawa T, Yokoyama K, Nakajima C, Suzuki Y, et al. Influence
350 of PD-L1 cross-linking on cell death in PD-L1-expressing cell lines and bovine
351 lymphocytes. *Immunology.* 2014;142: 5511317]27]561. doi:10.1111/imm.12243
- 352 6. Ikebuchi R, Konnai S, Shirai T, Sunden Y, Murata S, Onuma M, et al. Increase of cells
353 expressing PD-L1 in bovine leukemia virus infection and enhancement of anti-viral
354 immune responses in vitro via PD-L1 blockade. *Vet Res.* 2011;42: 103. doi:10.1186/1297-
355 9716-42-103
- 356 7. Ikebuchi R, Konnai S, Okagawa T, Yokoyama K, Nakajima C, Suzuki Y, et al. Blockade
357 of bovine PD-1 increases T cell function and inhibits bovine leukemia virus expression in
358 B cells in vitro. *Vet Res.* 2013;44: 59. doi:10.1186/1297-9716-44-59
- 359 8. Okagawa T, Konnai S, Nishimori A, Ikebuchi R, Mizorogi S, Nagata R, et al. Bovine
360 immunoinhibitory receptors contribute to the suppression of *Mycobacterium avium* subsp.
361 paratuberculosis-specific T-cell responses. *Infect Immun.* 2016;84: 77–89.

- 362 doi:10.1128/IAI.01014-15
- 363 9. Okagawa T, Konnai S, Deringer JR, Ueti MW, Scoles GA, Murata S, et al. Cooperation of
364 PD-1 and LAG-3 contributes to T-cell exhaustion in *Anaplasma marginale*-infected cattle.
365 Infect Immun. 2016;84: 2779–2790. doi:10.1128/IAI.00278-16
- 366 10. Goto S, Konnai S, Okagawa T, Nishimori A, Maekawa N, Gondaira S, et al. Increase of
367 cells expressing PD-1 and PD-L1 and enhancement of IFN- γ production via PD-1/PD-L1
368 blockade in bovine mycoplasmosis. Immunity, Inflamm Dis. 2017;5: 355–363.
369 doi:10.1002/iid3.173
- 370 11. Maekawa N, Konnai S, Ikebuchi R, Okagawa T, Adachi M, Takagi S, Kagawa Y,
371 Nakajima C, Suzuki Y, Murata S, et al. Expression of PD-L1 on canine tumor cells and
372 enhancement of IFN- γ production from tumor-infiltrating cells by PD-L1 blockade. *PLoS*
373 *One* (2014) **9**:e98415. doi:10.1371/journal.pone.0098415
- 374 12. Maekawa N, Konnai S, Ikebuchi R, Okagawa T, Adachi M, Takagi S, et al. Expression of
375 PD-L1 on canine tumor cells and enhancement of IFN- γ production from tumor-infiltrating
376 cells by PD-L1 blockade. *PLoS One*. 2014;9: e98415. doi:10.1371/journal.pone.0098415
- 377 13. Nishimori A, Konnai S, Okagawa T, Maekawa N, Ikebuchi R, Goto S, et al. In vitro and
378 in vivo antiviral activity of an anti-programmed death-ligand 1 (PD-L1) rat-bovine
379 chimeric antibody against bovine leukemia virus infection. *PLoS One*. 2017;12: e0174916.
380 doi:10.1371/journal.pone.0174916
- 381 14. Okagawa T, Konnai S, Nishimori A, Maekawa N, Ikebuchi R, Goto S, et al. Anti-bovine
382 programmed death-1 rat-bovine chimeric antibody for immunotherapy of bovine leukemia
383 virus infection in cattle. *Front Immunol*. 2017;8: 650. doi:10.3389/fimmu.2017.00650
- 384 15. Sajiki Y, Konnai S, Okagawa T, Nishimori A, Maekawa N, Goto S, et al. Prostaglandin

- 385 E2-Induced Immune Exhaustion and Enhancement of Antiviral Effects by Anti-PD-L1
386 Antibody Combined with COX-2 Inhibitor in Bovine Leukemia Virus Infection. *J*
387 *Immunol.* 2019;203: 1313–1324. doi:10.4049/jimmunol.1900342
- 388 16. Goto S, Konnai S, Hirano Y, Kohara J, Okagawa T, Maekawa N, Sajiki Y, Watari K,
389 Minato E, Kobayashi A, et al. Clinical efficacy of the combined treatment of antiPD-L1
390 rat-bovine chimeric antibody with a COX-2 inhibitor in calves infected with *Mycoplasma*
391 *bovis*. *Jpn J Vet Res.* in press
- 392 17. Maekawa N, Konnai S, Takagi S, Kagawa Y, Okagawa T, Nishimori A, et al. A canine
393 chimeric monoclonal antibody targeting PD-L1 and its clinical efficacy in canine oral
394 malignant melanoma or undifferentiated sarcoma. *Sci Rep.* 2017;7: 8951.
395 doi:10.1038/s41598-017-09444-2
- 396 18. Kumar S, Stecher G, Tamura K. MEGA7: Molecular Evolutionary Genetics Analysis
397 version 7.0 for bigger datasets. *Mol Biol Evol.* 2016;33: msw054.
398 doi:10.1093/molbev/msw054
- 399 19. Niwa H, Yamamura K, Miyazaki J. Efficient selection for high-expression transfectants
400 with a novel eukaryotic vector. *Gene.* 1991;108: 193–199. doi:10.1016/0378-
401 1119(91)90434-D
- 402 20. Sajiki Y, Konnai S, Okagawa T, Nishimori A, Maekawa N, Goto S, et al. Prostaglandin E2
403 induction suppresses the Th1 immune responses in cattle with Johne's disease. *Infect*
404 *Immun.* 2018;86: e00910-17. doi:10.1128/IAI.00910-17
- 405 21. O'Malley DP, Yang Y, Boisot S, Sudarsanam S, Wang JF, Chizhevsky V, et al.
406 Immunohistochemical detection of PD-L1 among diverse human neoplasms in a reference
407 laboratory: observations based upon 62,896 cases. *Mod Pathol.* 2019;32: 929–942.

- 408 doi:10.1038/s41379-019-0210-3
- 409 22. Brosnahan MM, Paradis MR. Demographic and clinical characteristics of geriatric horses:
410 467 cases (1989-1999). *J Am Vet Med Assoc.* 2003;223: 93–98.
411 doi:10.2460/javma.2003.223.93
- 412 23. Welsh CE, Duz M, Parkin TDH, Marshall JF. Prevalence, survival analysis and
413 multimorbidity of chronic diseases in the general veterinarian-attended horse population of
414 the UK. *Prev Vet Med.* 2016;131: 137–145. doi:10.1016/j.prevetmed.2016.07.011
- 415 24. Valentine BA. Survey of Equine Cutaneous Neoplasia in the Pacific Northwest. *J Vet*
416 *Diagnostic Investig.* 2006;18: 123–126. doi:10.1177/104063870601800121
- 417 25. Topalian SL, Hodi FS, Brahmer JR, Gettinger SN, Smith DC, McDermott DF, et al. Safety,
418 Activity, and Immune Correlates of Anti-PD-1 Antibody in Cancer. *N Engl J Med.*
419 2012;366: 2443–2454. doi:10.1056/NEJMoa1200690
- 420 26. Brahmer JR, Tykodi SS, Chow LQM, Hwu W-J, Topalian SL, Hwu P, et al. Safety and
421 activity of anti-PD-L1 antibody in patients with advanced cancer. *N Engl J Med.* 2012;366:
422 2455–2465. doi:10.1056/NEJMoa1200694
- 423 27. Sun C, Mezzadra R, Schumacher TN. Regulation and Function of the PD-L1 Checkpoint.
424 *Immunity.* 2018;48: 434–452. doi:10.1016/j.immuni.2018.03.014
- 425 28. Rosengren Pielberg G, Golovko A, Sundström E, Curik I, Lennartsson J, Seltenhammer
426 MH, et al. A cis-acting regulatory mutation causes premature hair graying and
427 susceptibility to melanoma in the horse. *Nat Genet.* 2008;40: 1004–1009.
428 doi:10.1038/ng.185
- 429 29. Jiang L, Campagne C, Sundström E, Sousa P, Imran S, Seltenhammer M, et al. Constitutive
430 activation of the ERK pathway in melanoma and skin melanocytes in Grey horses. *BMC*

- 431 Cancer. 2014;14: 1–11. doi:10.1186/1471-2407-14-857
- 432 30. Smalley KSM. A pivotal role for ERK in the oncogenic behaviour of malignant melanoma?
433 Int J Cancer. 2003;104: 527–532. doi:10.1002/ijc.10978
- 434 31. Jiang X, Zhou J, Giobbie-Hurder A, Wargo J, Hodi FS. The activation of MAPK in
435 melanoma cells resistant to BRAF inhibition promotes PD-L1 expression that is reversible
436 by MEK and PI3K inhibition. Clin Cancer Res. 2013;19: 598–609. doi:10.1158/1078-
437 0432.CCR-12-2731
- 438 32. Liu J, Hamrouni A, Wolowiec D, Coiteux V, Kuliczowski K, Hetuin D, et al. Plasma cells
439 from multiple myeloma patients express B7-H1 (PD-L1) and increase expression after
440 stimulation with IFN- γ and TLR ligands via a MyD88-, TRAF6-, and MEK-dependent
441 pathway. Blood. 2007;110: 296–304. doi:10.1182/blood-2006-10-051482
- 442 33. Liu L, Mayes PA, Eastman S, Shi H, Yadavilli S, Zhang T, et al. The BRAF and MEK
443 inhibitors dabrafenib and trametinib: Effects on immune function and in combination with
444 immunomodulatory antibodies targeting PD-1, PD-L1, and CTLA-4. Clin Cancer Res.
445 2015;21: 1639–1651. doi:10.1158/1078-0432.CCR-14-2339
- 446

447 **Figure Legends**

448 **Figure 1. Sequence analysis of EqPD-1**

449 (A) Multiple sequence alignment of amino acid sequences of equine and vertebrate PD-1.
450 Predicted domains and motifs of EqPD-1 are shown. EqPD-1 consists of a signal peptide, an
451 extracellular region, a transmembrane region, and an intracellular region. The cytoplasmic tail of
452 PD-1 contains the ITIM and ITSM motifs. (B) Phylogenetic tree of EqPD-1 sequence in relation
453 to those of other vertebrate species. The bootstrap consensus tree was inferred from 1000 replicates
454 with the neighbor-joining method using the MEGA 7.0 software. The scale indicates the
455 divergence time. The GenBank accession numbers of nucleotide sequences used in these analyses
456 are listed in Supplementary Table 3.

457 **Figure 2. Sequence analysis of EqPD-L1**

458 (A) Multiple sequence alignment of PD-L1 amino acid sequences of equine and vertebrate PD-1.
459 Predicted domains and motifs of EqPD-L1 are shown in the figure. EqPD-L1 consists of a signal
460 peptide, an extracellular region, a transmembrane region, and an intracellular region. (B)
461 Phylogenetic tree of the EqPD-L1 sequence in relation to other vertebrate species. The bootstrap
462 consensus tree was inferred from 1000 replicates with the neighbor-joining method using the
463 MEGA 7.0 software. The scale indicates the divergence time. The GenBank accession numbers of
464 nucleotide sequences used in these analyses are listed in Supplementary Table 3.

465 **Figure 3. Establishment of EqPD-1- or EqPD-L1-expressing cells and Ig fusion soluble**
466 **proteins.**

467 (A) EqPD-1-EGFP or EqPD-L1-EGFP-expressing COS-7 cell. The subcellular distributions of
468 EqPD-1-EGFP and EqPD-L1-EGFP in transfected COS-7 cells were analyzed using a
469 fluorescence microscope. (B) Production and purification of Ig fusion EqPD-1 and EqPD-L1

470 proteins. EqPD-1-Ig and EqPD-L1-Ig were purified from the culture supernatant and analyzed
471 with SDS-PAGE. (C) Interaction of EqPD-1 and EqPD-L1. EqPD-1-EGFP or EqPD-L1-
472 expressing COS-7 cells were incubated with EqPD-L1-Ig or EqPD-1-Ig, respectively. The binding
473 of the Ig fusion proteins was labeled using Alexa Flour 647 conjugated anti-rabbit IgG antibody
474 and analyzed by flow cytometry.

475 **Figure 4. Cross-reactivity of anti-bovine PD-L1 mAbs against EqPD-L1.**

476 (A–C) Binding activities of anti-bovine PD-L1 mAbs (5A2-A1, 6C11-3A11, 4G12-C1, and 6G7-
477 E1) to (A) EqPD-L1-EGFP-expressing COS-7 cells, (B) fresh equine PBMCs, and (C) equine
478 PBMCs stimulated with PMA and ionomycin for 24 h. The binding of the primary mAbs was
479 labeled with APC conjugated anti-rat Ig antibody and analyzed by flow cytometry. Rat IgG₁ and
480 IgG_{2a} controls were used as isotype-matched negative controls.

481 **Figure 5. Inhibition of equine PD-1/PD-L1 binding by anti-PD-L1 mAbs.**

482 The blocking effect of anti-PD-L1 mAb on the binding of EqPD-L1-Ig to EqPD-1-Ig. EqPD-1-Ig
483 was coated on a microwell plate. Biotinylated EqPD-L1-Ig was preincubated with various
484 concentrations of anti-PD-L1 mAb (5A2-A1 or 6C11-3A11), and then incubated in the coated
485 microwell plate. Rat IgG₁ and IgG_{2a} controls were used as isotype-matched negative controls. Each
486 curve represents the relative binding of EqPD-L1-Ig preincubated with antibodies compared to no-
487 antibody control. Each point indicates the average value of three independent experiments.
488 Significant differences between each treatment were identified using Tukey's test. An asterisk (*)
489 indicates $p < 0.05$.

490 **Figure 6. Immunohistochemical analysis of PD-L1 in EMM.**

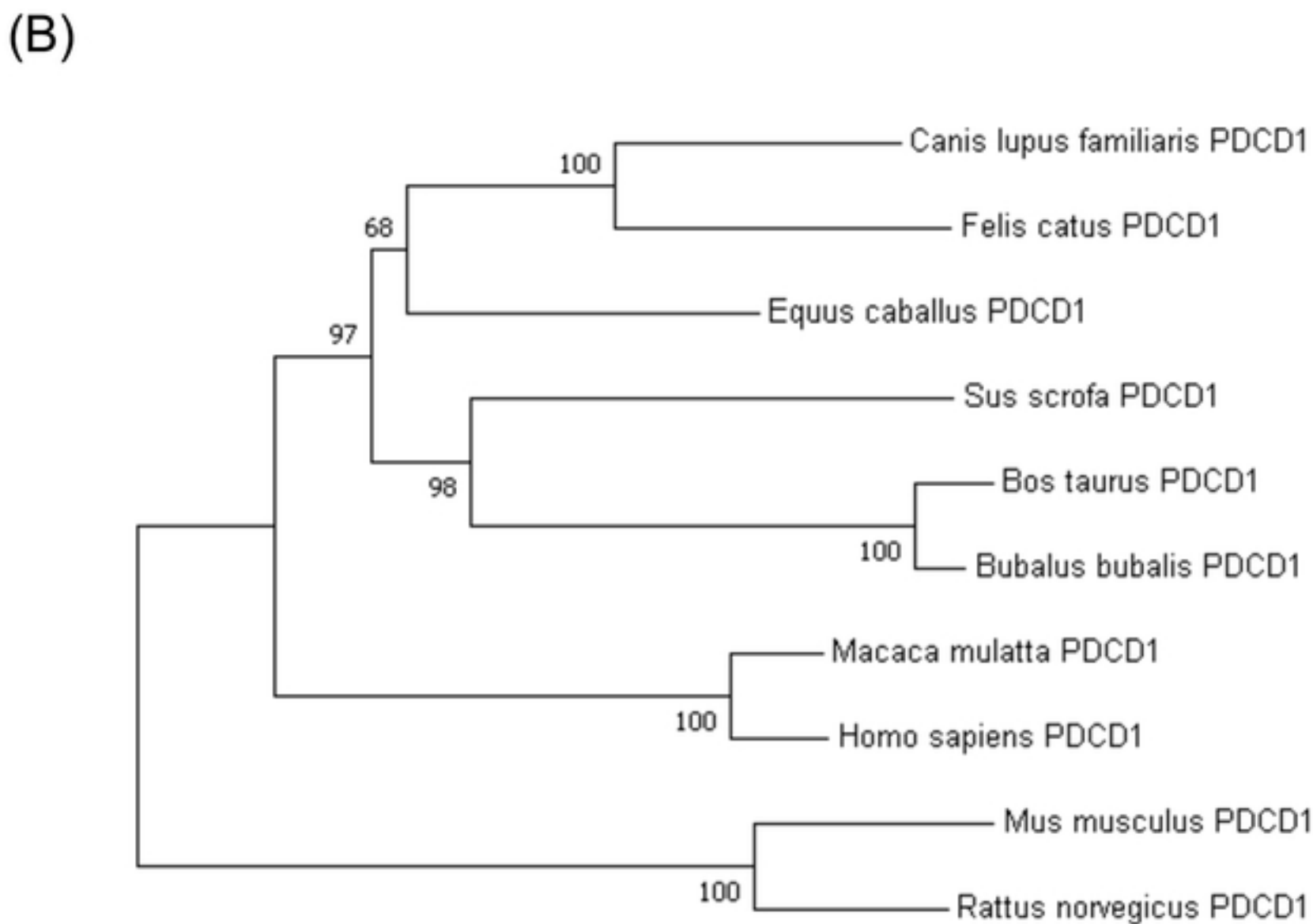
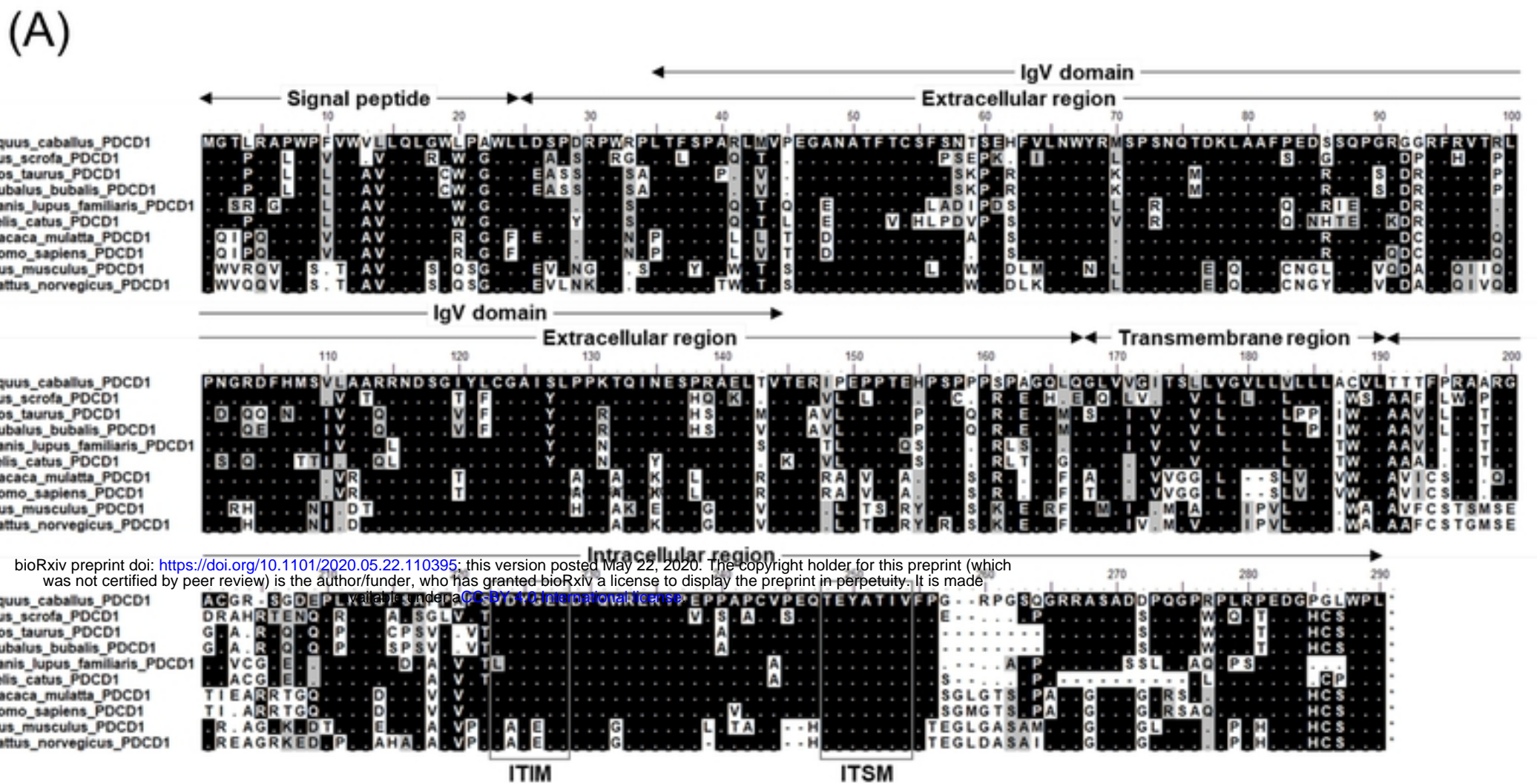
491 Immunohistochemical staining of PD-L1 in tumor tissues of horses with melanoma (#1–#4). Each
492 section was stained (A) without a primary antibody (control) or (B) using anti-bovine PD-L1 mAb
493 (6C11-3A11). Further information of tumor specimens is shown in Supplementary Table 2.

494 **Figure 7. Effect of PD-L1 blockade on IFN- γ and IL-2 production.**

495 PBMCs isolated from healthy horses were cultured with anti-PD-L1 mAb (6C11-3A11) or rat
496 IgG_{2a} control in the presence of SEB. The culture supernatants were harvested three days later and
497 IFN- γ and IL-2 concentrations were measured by ELISA (IFN- γ : $n = 14$ and IL-2: $n = 9$).
498 Significant differences between each treatment were identified using Wilcoxon signed-rank test.
499 Asterisks (* and **) indicate $p < 0.05$ and < 0.01 , respectively.

500

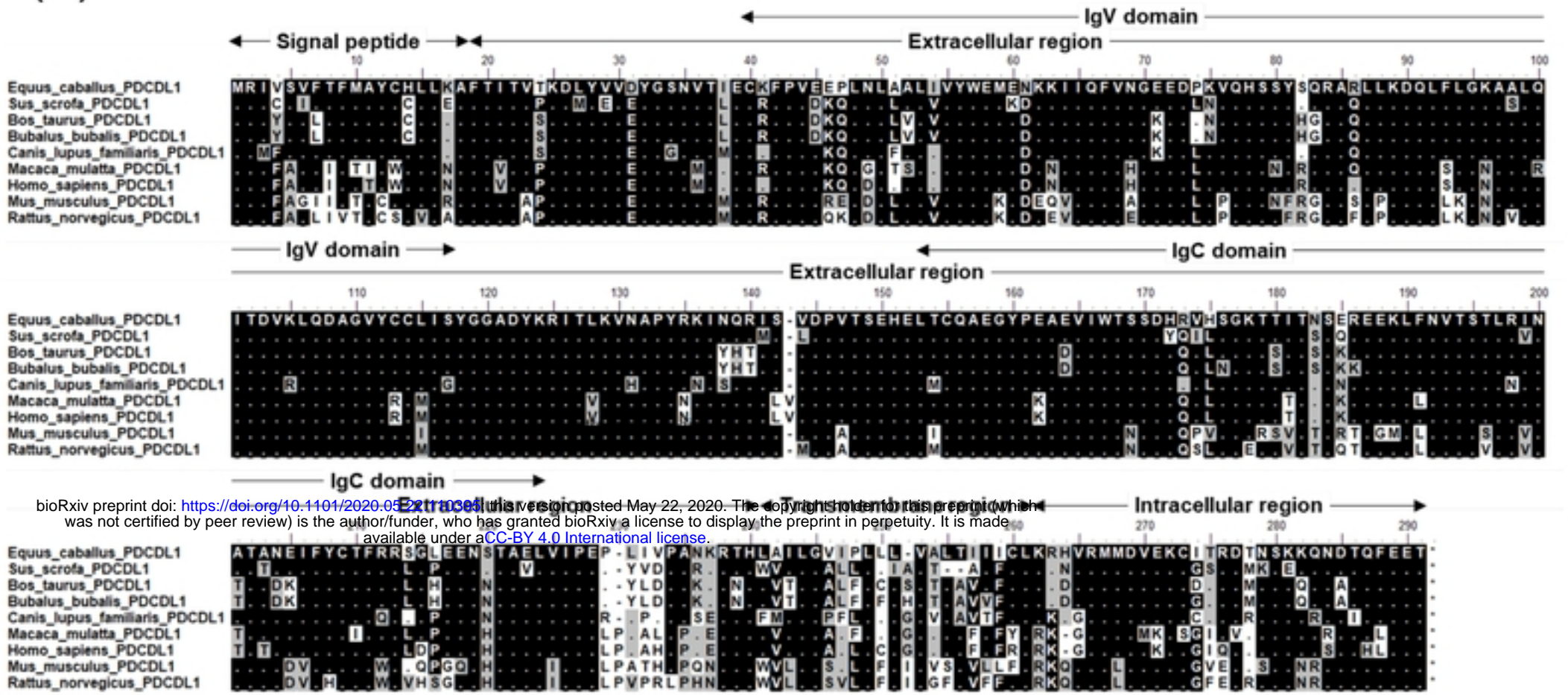
Figure 1



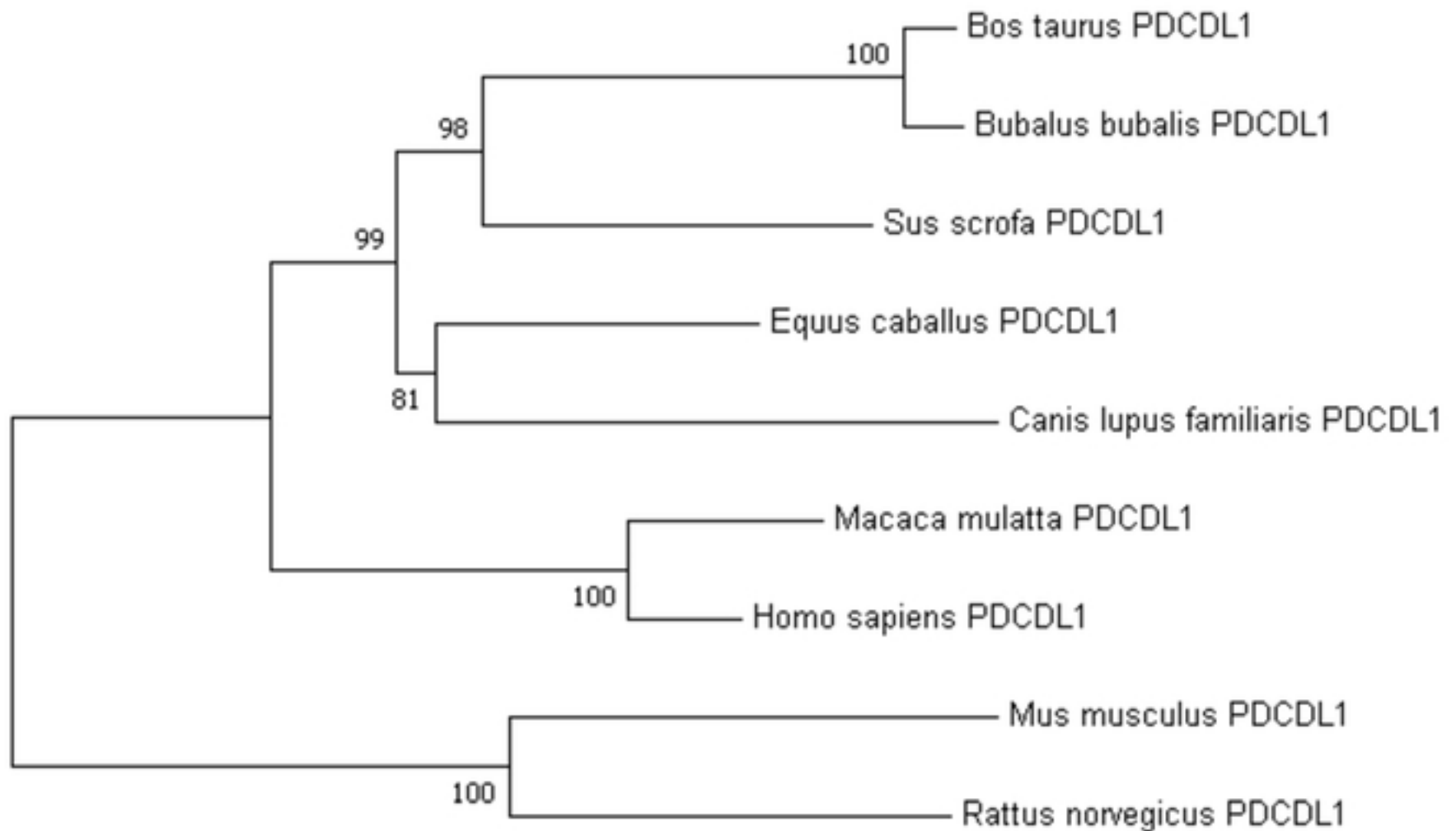
20

Figure 2

(A)



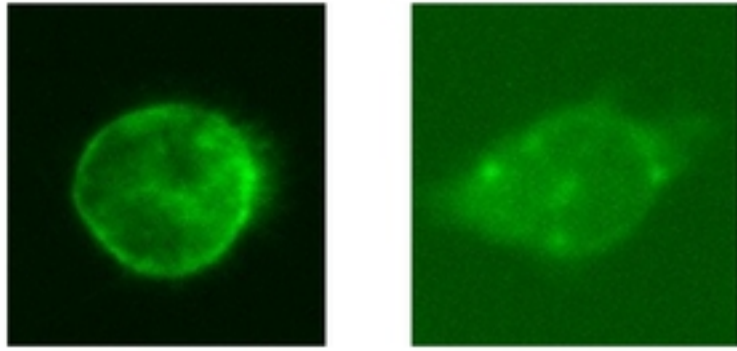
(B)



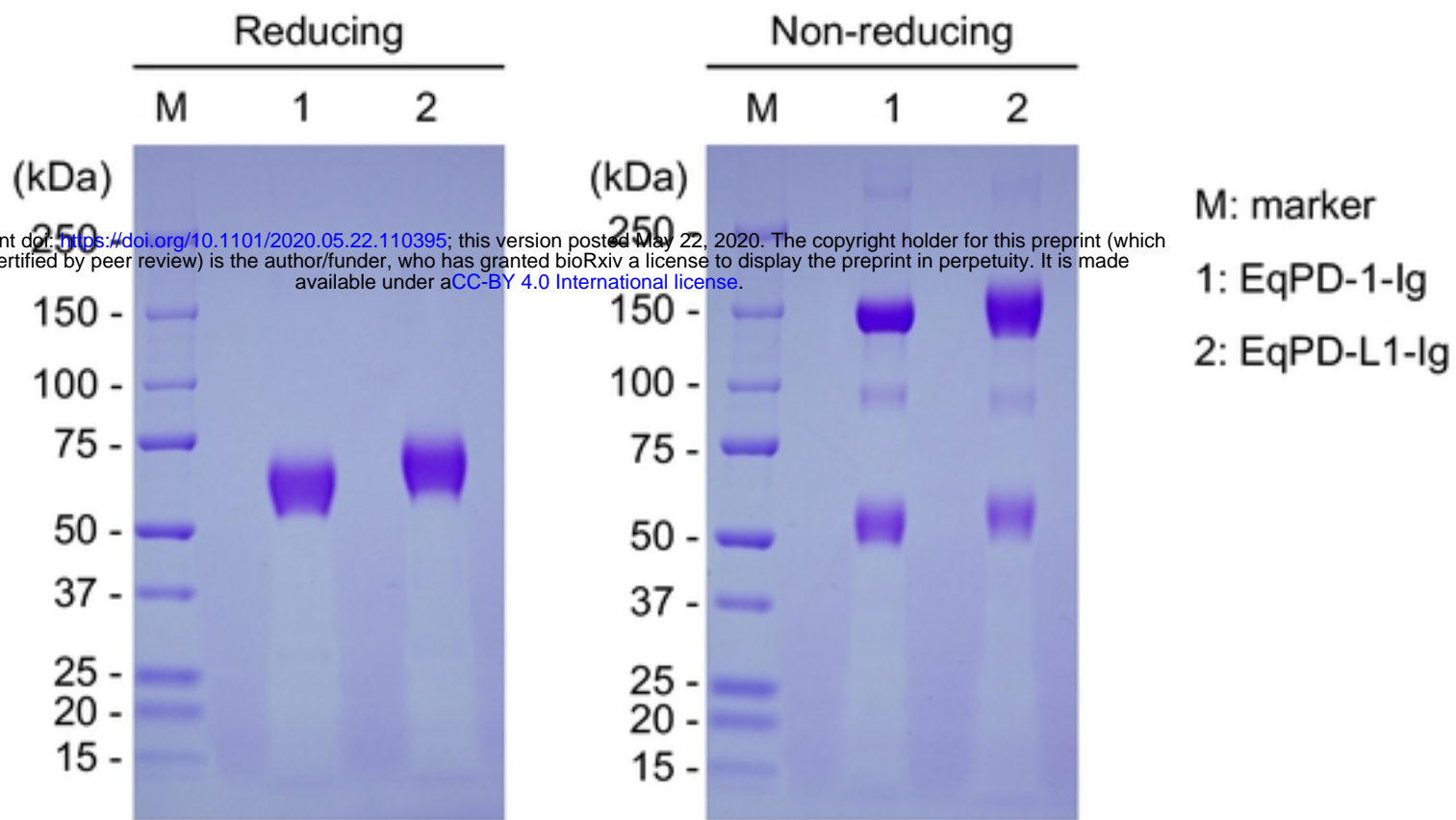
20

Figure 3

(A) EqpD-1-EGFP COS-7 cell EqpD-L1-EGFP COS-7 cell



(B)



(C)

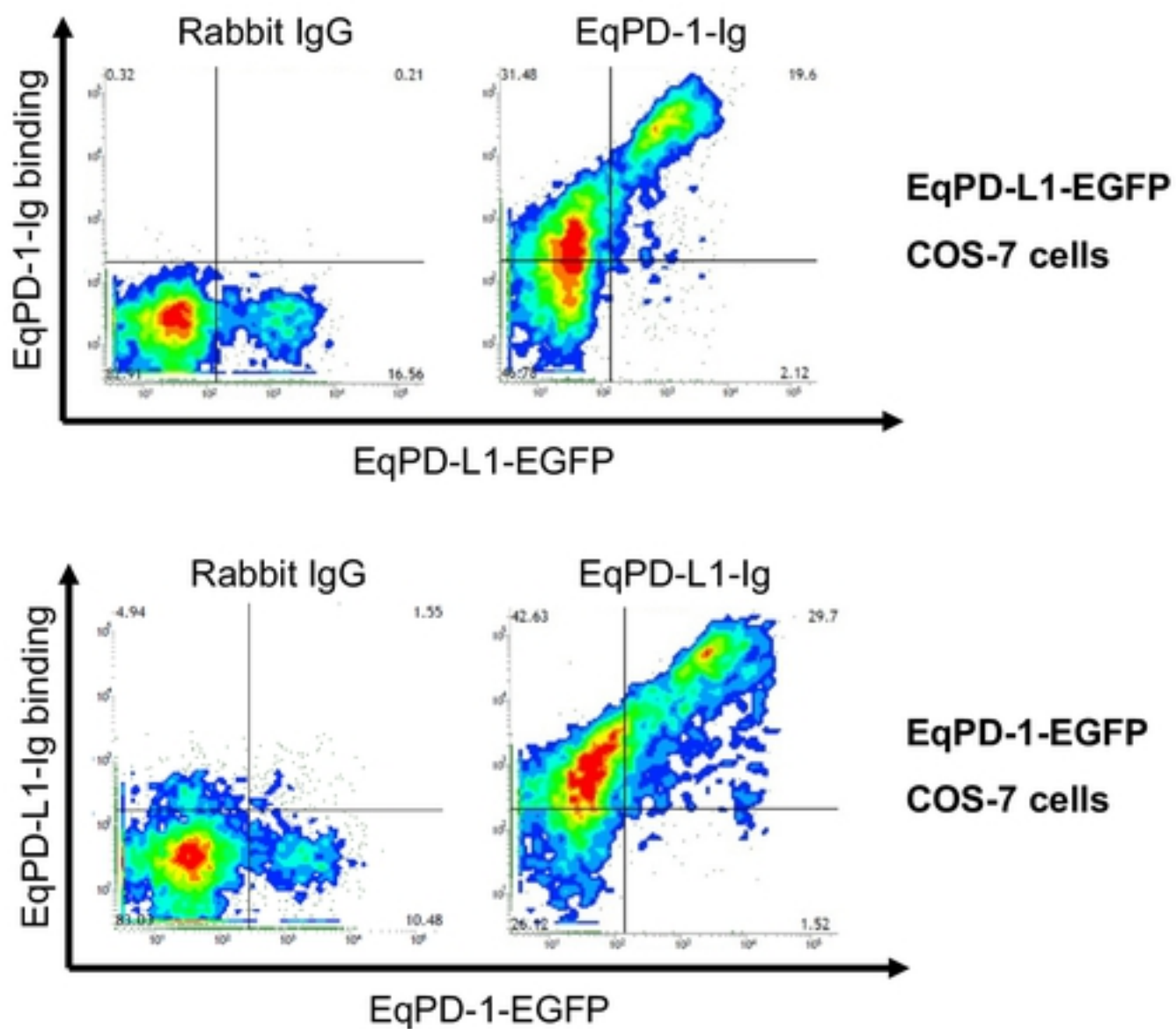
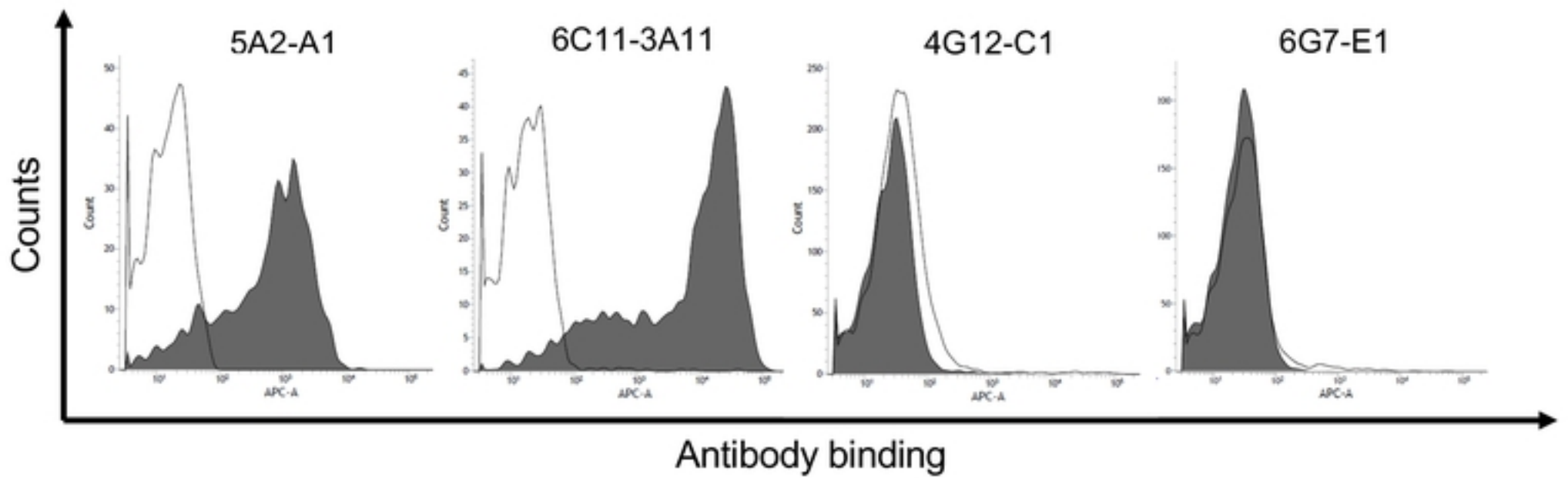


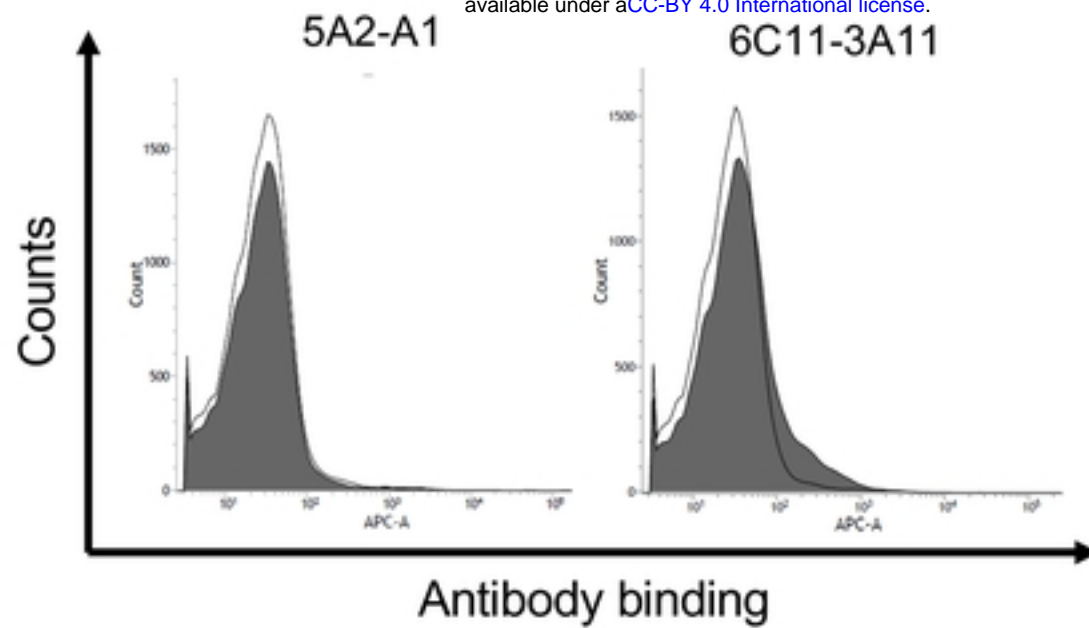
Figure 4

(A) EqPD-L1-EGFP-expressing COS-7 cells



(B) Fresh equine PBMCs

bioRxiv preprint doi: <https://doi.org/10.1101/2020.05.22.110395>; this version posted May 22, 2020. The copyright holder for this preprint (which was not certified by peer review) is the author/funder, who has granted bioRxiv a license to display the preprint in perpetuity. It is made available under aCC-BY 4.0 International license.



(C) Stimulated equine PBMCs

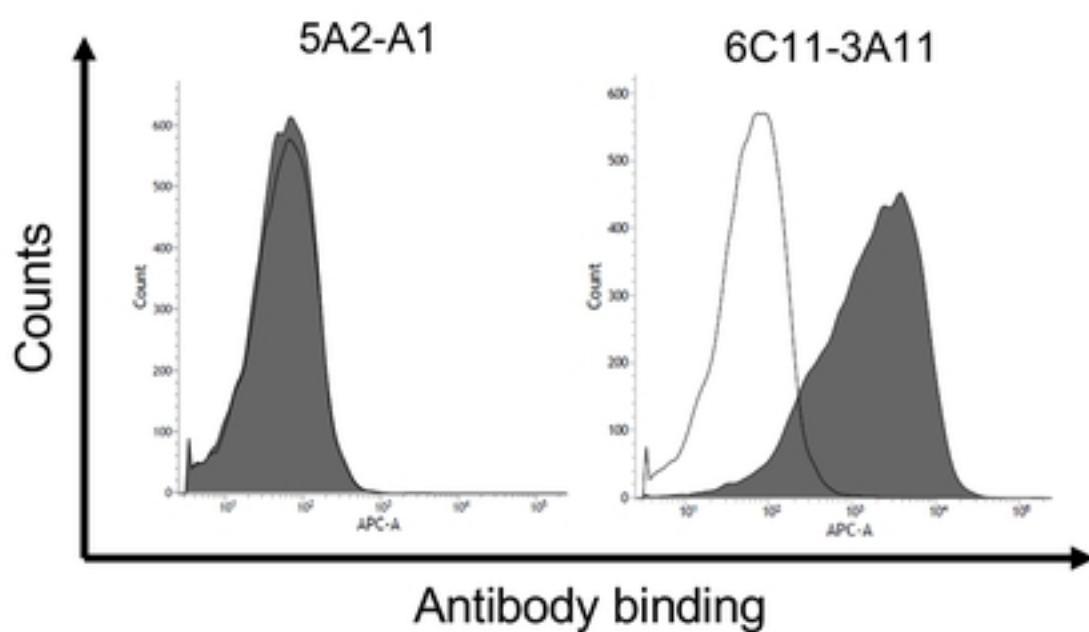


Figure 5

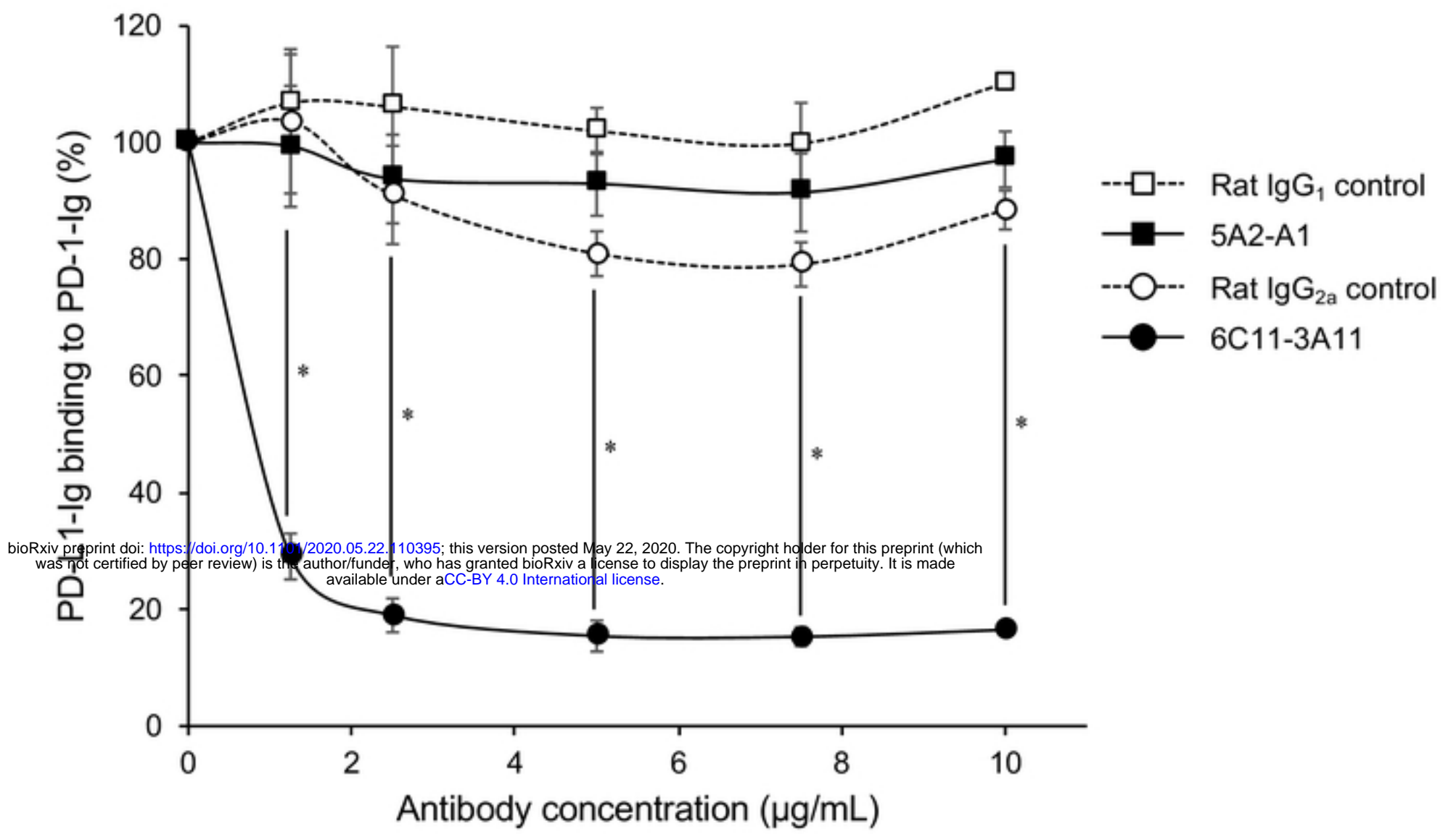
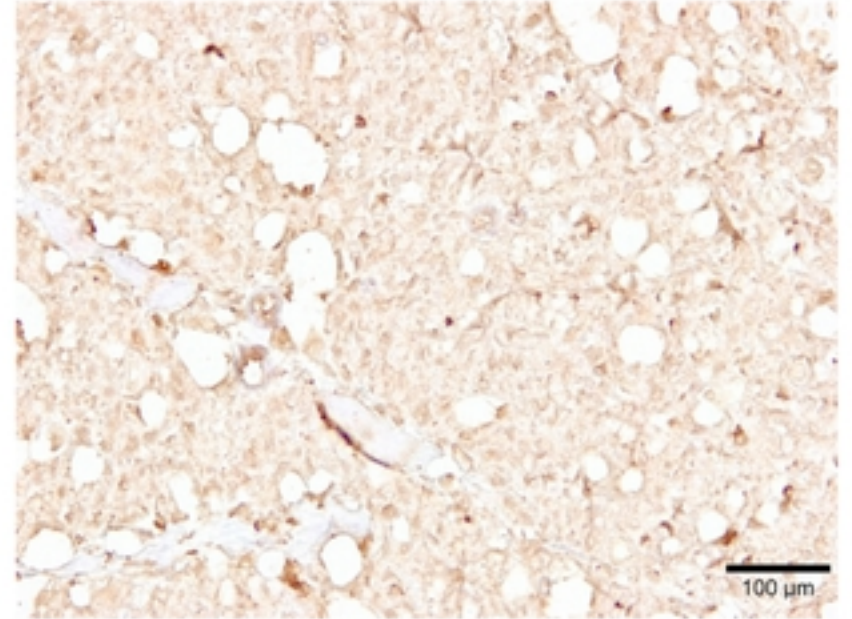
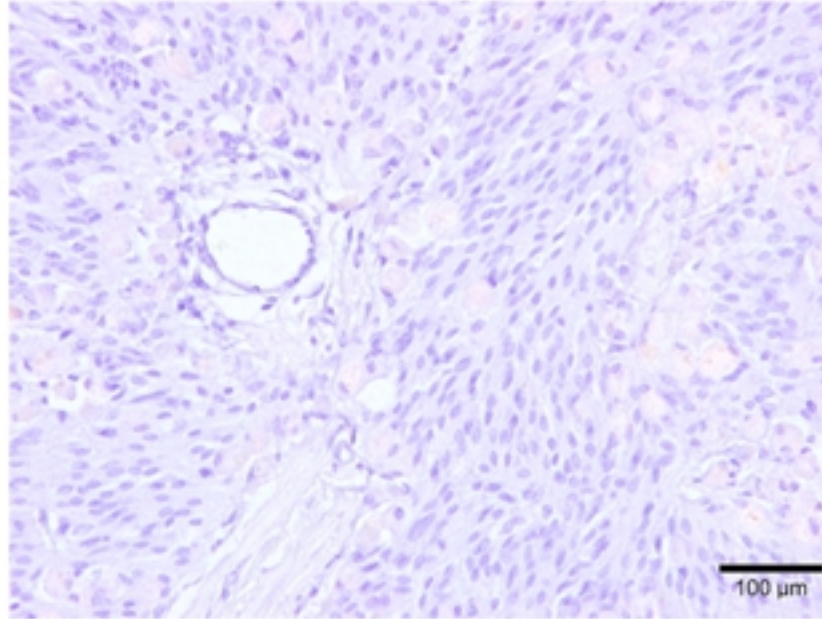


Figure 6

(A) Control

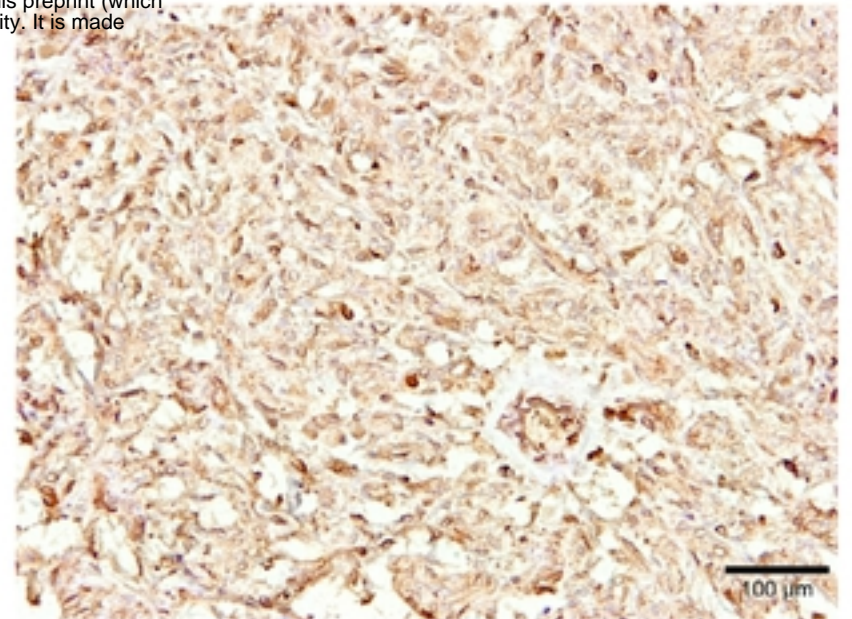
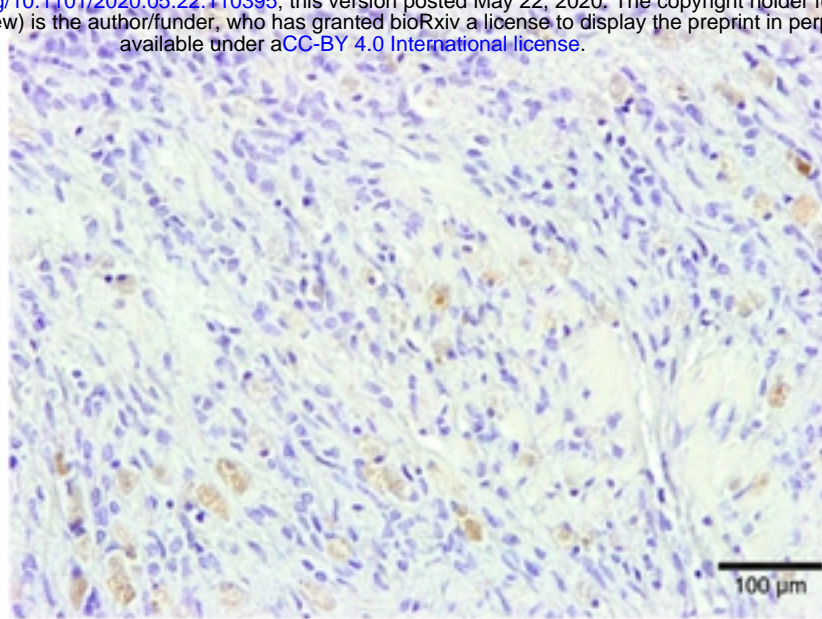
(B) PD-L1

Equine melanoma #1 (esophagus)

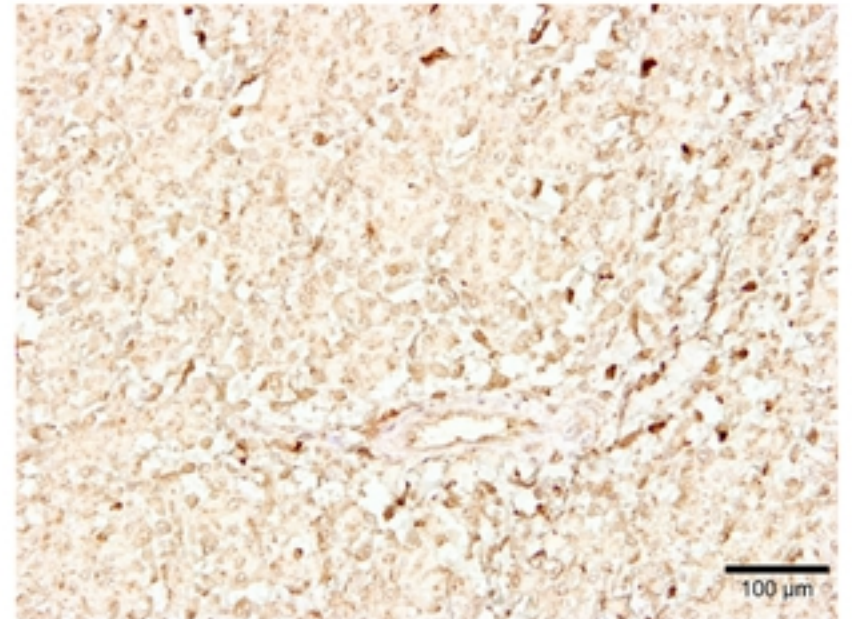
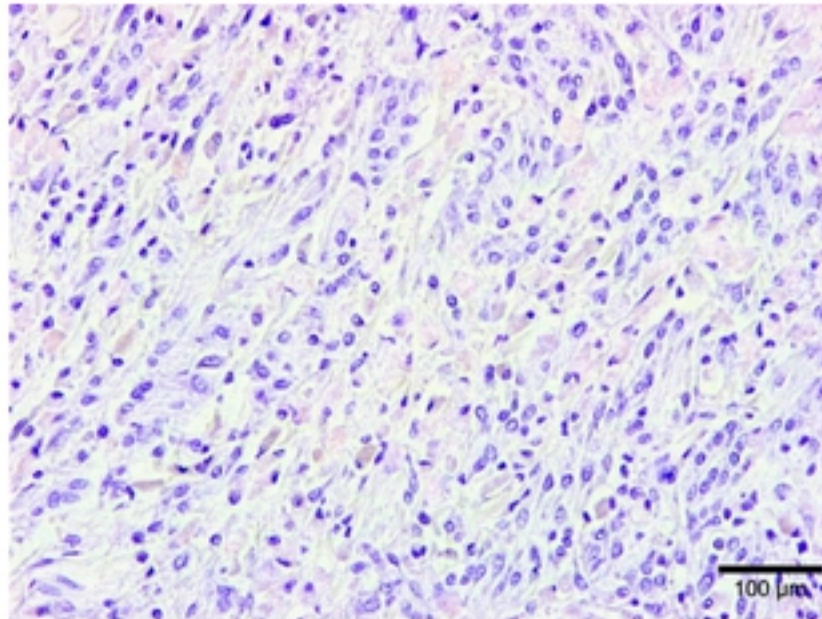


bioRxiv preprint doi: <https://doi.org/10.1101/2020.05.22.110395>; this version posted May 22, 2020. The copyright holder for this preprint (which was not certified by peer review) is the author/funder, who has granted bioRxiv a license to display the preprint in perpetuity. It is made available under aCC-BY 4.0 International license.

Equine melanoma #2 (skin)



Equine melanoma #3 (skin)



Equine melanoma #4 (skin)

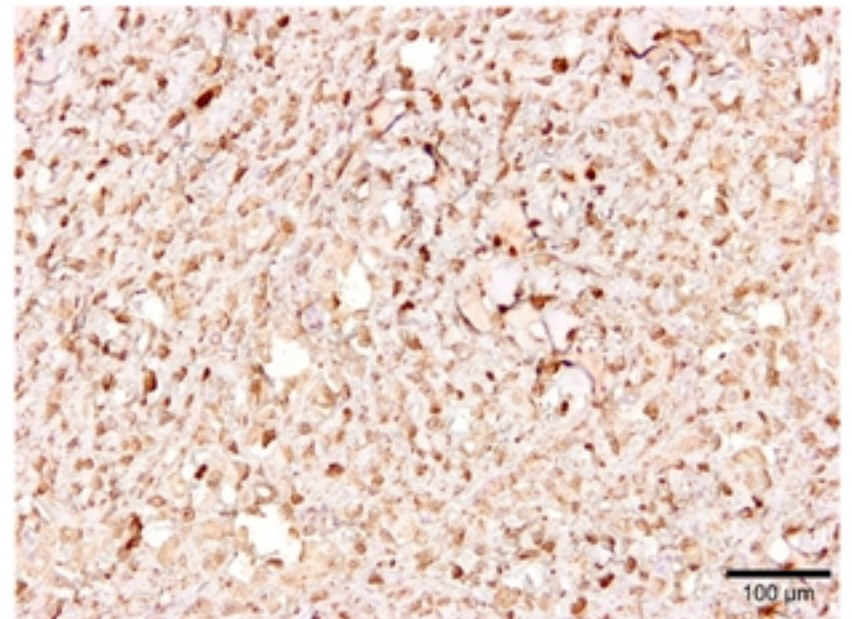
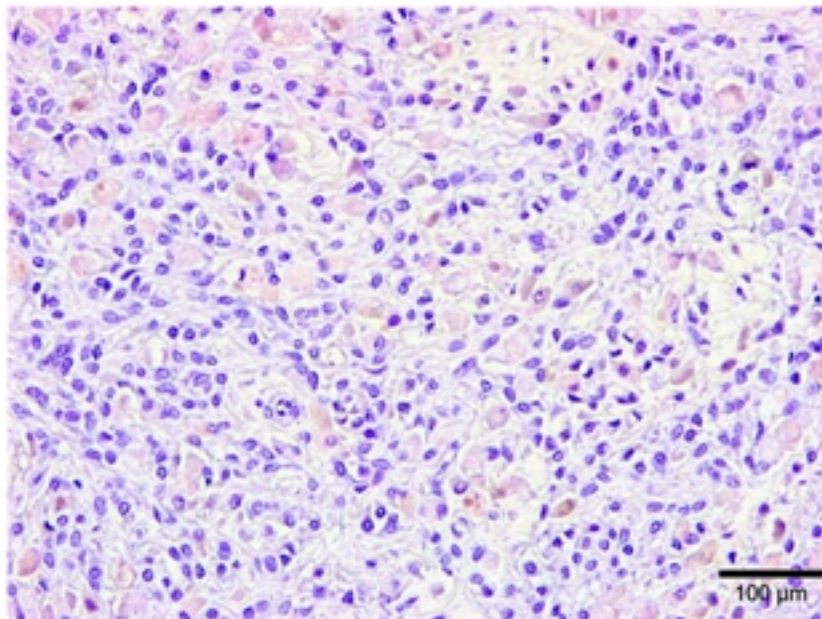
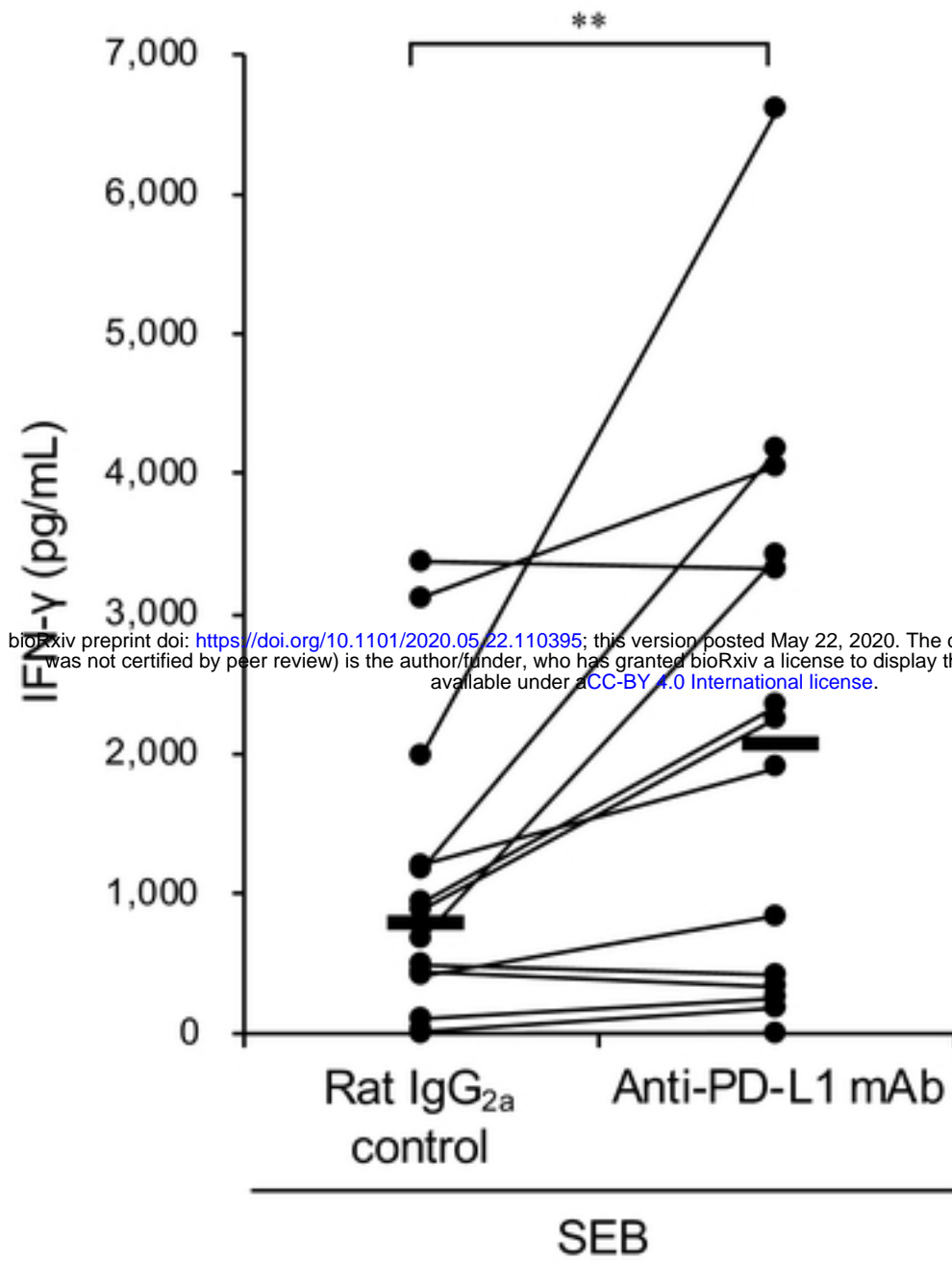


Figure 7

(A) IFN- γ production



(B) IL-2 production

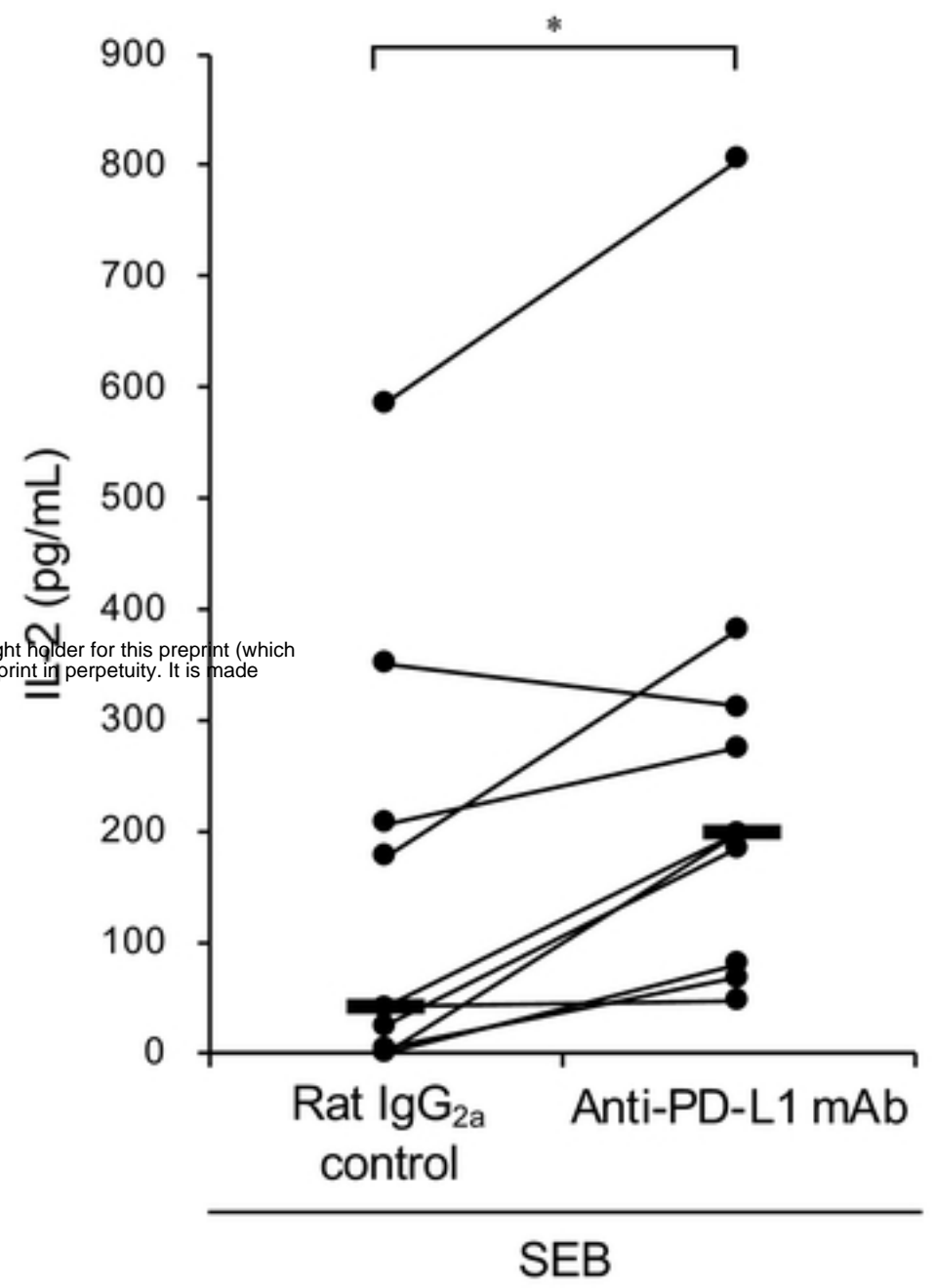


Table 1. Similarities of nucleotide and amino acid sequences of PD-1 among mammalian species

	Horse	Pig	Cattle	Water buffalo	Dog	Cat	Human	Monkey	Mouse	Rat
Horse	-	82.5	79.1	79.3	83.3	80.5	79.7	80.3	72.4	73.1
Pig	70.4	-	85.2	80.8	78.5	78.5	76.8	76.7	69.6	70.8
Cattle	69.0	71.5	-	97.5	78.3	78.3	74.5	74.7	68.5	67.8
Water buffalo	70.8	73.2	96.8	-	78.8	78.6	74.5	75.2	69.5	68.4
Dog	75.6	67.9	69.3	71.0	-	88.3	76.7	77.2	70.4	71.5
Cat	72.2	65.2	69.7	71.1	82.2	-	76.4	75.9	69.8	70.8
Human	69.2	63.7	63.7	63.4	65.3	62.4	-	95.8	71.7	72.5
Monkey	70.6	64.1	65.1	65.8	65.3	62.0	95.8	-	71.6	72.5
Mouse	58.7	55.1	51.3	53.1	56.5	51.7	59.3	60.0	-	91.3
Rat	61.5	58.3	56.8	59.0	58.2	54.1	58.9	61.3	85.7	-

bioRxiv preprint doi: <https://doi.org/10.1101/2020.05.22.110395>; this version posted May 22, 2020. The copyright holder for this preprint (which was not certified by peer review) is the author/funder, who has granted bioRxiv a license to display the preprint in perpetuity. It is made available under aCC-BY 4.0 International license.

Upper section; similarities (%) in nucleotide level, lower section; similarities (%) in amino acid level.

Table 2. Similarities of nucleotide and amino acid sequences of PD-L1 among mammalian species

	Horse	Pig	Cattle	Water buffalo	Dog	Human	Monkey	Mouse	Rat
Horse	-	86.8	87.9	87.9	88.1	86.6	85.2	75.6	75.7
Pig	81.5	-	88.1	88.2	85.1	84.3	83.3	74.4	75.5
Cattle	80.9	81.3	-	98.2	84.0	83.0	81.8	73.8	75.2
Water buffalo	79.9	80.6	96.5	-	83.7	82.3	81.5	74.2	75.7
Dog	83.7	76.8	78.5	77.8	-	83.2	82.1	73.4	74.5
Human	79.0	73.3	73.1	72.0	75.9	-	95.7	76.3	76.4
Monkey	76.6	71.6	72.7	72.0	74.2	91.3	-	75.2	75.3
Mouse	67.9	67.4	65.1	66.2	67.0	69.4	68.3	-	87.3
Rat	68.3	67.4	67.3	67.6	68.1	69.7	68.3	83.4	-

Upper section; similarities (%) in nucleotide level, lower section; similarities (%) in amino acid level.